

Experimental determination of correlations for mean heat transfer coefficients in plate fin and tube heat exchangers

DAWID TALER*

Institute of Heat Transfer Engineering and Air Protection, Faculty of Environmental Engineering, Cracow University of Technology, Warszawska 24, 31-155 Cracow, Poland

Abstract This paper presents a numerical method for determining heat transfer coefficients in cross-flow heat exchangers with extended heat exchange surfaces. Coefficients in the correlations defining heat transfer on the liquid- and air-side were determined using a nonlinear regression method. Correlation coefficients were determined from the condition that the sum of squared liquid and air temperature differences at the heat exchanger outlet, obtained by measurements and those calculated, achieved minimum. Minimum of the sum of the squares was found using the Levenberg-Marquardt method. The uncertainty in estimated parameters was determined using the error propagation rule by Gauss. The outlet temperature of the liquid and air leaving the heat exchanger was calculated using the analytical model of the heat exchanger.

Keywords: Heat transfer correlations; Tube and plate fin heat exchangers; Mathematical model

Nomenclature

A	–	area, m ²
A_f	–	fin surface area, m ²
A_{in}, A_o	–	inner and outer area of the bare tube, m ²
A_{mf}	–	tube outer surface area between fins, m ²

*E-mail address: dtaler@pk.edu.pl

A_{\min}	–	minimum free flow frontal area on the air side, m^2
A_{oval}	–	area of oval opening in the plate fin, m^2
$A_{w, \text{in}}$	–	cross-section area of the tube, m^2
c	–	specific heat, $\text{J}/(\text{kg K})$
\bar{c}	–	mean specific heat, $\text{J}/(\text{kg K})$
\mathbf{C}	–	matrix
d_h	–	hydraulic diameter of air flow passages, m
d_t	–	hydraulic diameter on the liquid side, $4 A_{w, \text{in}}/P_{\text{in}}$, m
\mathbf{D}	–	variance-covariance matrix with positive diagonal elements
h	–	convection heat transfer coefficient, $\text{W}/(\text{m}^2\text{K})$
h_o	–	weighted heat transfer coefficient, $\text{W}/(\text{m}^2\text{K})$
H_{ch}	–	height of automotive radiator, m
\mathbf{I}	–	identity matrix
\mathbf{J}	–	Jacobian matrix
k	–	thermal conductivity, $\text{W}/(\text{m K})$
k_t	–	tube thermal conductivity, $\text{W}/(\text{m K})$
(k)	–	iteration number
L	–	heat exchanger thickness, $L = 2p_2$, m
L_{ch}	–	length of automotive radiator, m
m	–	number of measured water and air temperatures (total number of data points is equal to 2 m)
\dot{m}	–	mass flow rate, kg/s
\dot{m}_a	–	air mass flow rate, kg/s
\dot{m}_w	–	water mass flow rate, kg/s
n	–	number of unknown parameters
n_l, n_u	–	number of tubes in the first row in the first (upper) and the second (lower) pass of heat exchanger, respectively
n_r	–	total number of tubes in the first row of heat exchanger, $n_r = n_l + n_u$
N_a, N_w	–	air and water number of transfer units, respectively
Nu_a	–	air side Nusselt number, $= h_a d_h/k_a$
Nu_w	–	water side Nusselt number, $= h_w d_t/k_w$
p_1	–	pitch of tubes in plane perpendicular to flow (fin height), m
p_2	–	pitch of tubes in direction of flow (fin width), m
P	–	confidence interval of the estimated parameters, %
P_{in}, P_o	–	inside and outside perimeter of the oval tube, respectively, m
Pr	–	Prandtl number, $= \mu c_p/k$
\dot{Q}	–	heat flow rate in exchanger between hot water and cold air, W
Re_a	–	air side Reynolds number, $= w_{\text{max}} d_h/\nu_a$
Re_w	–	water side Reynolds number, $= w_w d_t/\nu_w$
s	–	fin pitch, m
s_t^2	–	variance of the fit, K^2
S	–	sum of temperature difference squares, K^2
$t_{m-n}^{\alpha/2}$	–	the $(1 - \alpha/2)^{\text{th}}$ quantile of the Student's t -distribution for m data points and n unknown parameters with $m - n$ degrees of freedom,
T	–	temperature, $^{\circ}\text{C}$
\mathbf{T}''	–	vector of water and air temperatures at the outlet of the heat exchanger,
T_a	–	air temperature, $^{\circ}\text{C}$

T'_{am}, T''_{am}	– mean inlet and outlet temperature of air from the heat exchanger, °C
$T'_{lm}, T''_{lm}, T'''_{lm}$	– mean air temperature at inlet and after the first and second row of tubes at the second (lower) pass, respectively, °C (Fig. 1)
$T'_{um}, T''_{um}, T'''_{um}$	– mean air temperature at inlet, after the first, and second row of tubes at the first (upper) pass, respectively, °C (Fig. 1)
T_w	– water temperature, °C
T_{wm}	– water outlet temperature after the first pass, °C
T'_w, T''_w	– water inlet and outlet temperature, respectively, °C
$T'_{w,1}, T'_{w,2}$	– water temperature at the inlet to the first and second tube row in the first pass, °C (Fig. 1)
$T'_{w,3}, T'_{w,4}$	– water temperature at the inlet to the first and second tube row in the second pass, °C (Fig. 1)
$T''_{w,1}, T''_{w,2}$	– water temperature at the outlet from the first and second tube row in the first pass, °C (Fig. 1)
$T''_{w,3}, T''_{w,4}$	– water temperature at the outlet from the first and second tube row in the second pass, °C (Fig. 1)
U_o	– overall heat transfer coefficient related to the outer surface of bare tube, W/(m ² K)
\dot{V}'_a, \dot{V}'_w	– air and water volume flow rate before the heat exchanger, m ³ /s
w_a, w_w	– weighting factor for measured air and water temperature w_{\max} mean velocity in the minimum free flow area, m/s
w_0	– average frontal flow velocity, m/s
W	– matrix of weighting factors
x_1, \dots, x_n	– unknown parameters
x	– vector of unknown parameters
x, y, z	– Cartesian coordinates

Greek symbols

δ_f	– fin thickness, m
δ_t	– tube wall thickness, m
ε	– relative difference between water side and average heat flow rate, %
η_f	– fin efficiency
μ	– dynamic viscosity, Pa s
ν	– kinematic viscosity, m ² /s
ρ	– density, kg/m ³
σ_a^2	– variance of measured air temperature, K ²
σ_w^2	– variance of measured water temperature, K ²
ξ	– friction factor

Subscripts

a	– air
f	– fin
in	– inner
o	– outer
t	– tube
w	– water

Superscripts

<i>c</i>	–	calculated
<i>l</i>	–	lower pass (second pass)
<i>m</i>	–	measured
<i>u</i>	–	upper pass
–	–	mean

1 Introduction

Most engineering calculations of heat transfer in heat exchangers use heat transfer coefficients obtained from experimental data. The empirical approach involves performing heat transfer measurements and correlating the data in terms of appropriate dimensionless numbers, which are obtained from expressing mass, momentum, and energy conservation equations in dimensional forms or from the dimensionless analysis. A functional form of the Nusselt relationship

$$\text{Nu} = f(\text{Re}, \text{Pr}) \quad (1)$$

is usually based on energy and momentum-transfer analogies. Traditional expressions for calculation of heat transfer coefficient in fully developed flow in smooth tubes are usually products of two power functions of the Reynolds and Prandtl numbers. The Chilton-Colburn analogy written as [1]

$$j = \frac{\xi}{8}, \quad (2)$$

where

$$j = \frac{\text{Nu}}{\text{RePr}^{1/3}} \quad (3)$$

denotes the Colburn factor, can be used to find empirical equation for Nusselt number [1].

Substituting the Moody equation for the friction factor for smooth pipes [2,3]

$$\xi = \frac{0.184}{\text{Re}^{0.2}} \quad (4)$$

into Eq. (3) we obtain the relation proposed by Colburn

$$\text{Nu} = 0.023\text{Re}^{0.8}\text{Pr}^{1/3}, \quad 0.7 \leq \text{Pr} \leq 160, \quad \text{Re} \geq 10^4, \quad L/d \geq 60. \quad (5)$$

Similar correlation was developed by Dittus and Boelter [1,2,4]

$$\text{Nu} = 0.023\text{Re}^{0.8}\text{Pr}^n, \quad 0.7 \leq \text{Pr} \leq 100, \quad \text{Re} \geq 10^4, \quad L/d \geq 60, \quad (6)$$

where $n = 0.4$ if the fluid is being heated, and $n = 0.3$ if the fluid is being cooled.

A better accuracy of determining the heat transfer coefficient, h , can be achieved applying the Prandtl analogy [5,6]

$$\text{Nu} = \frac{\frac{\xi}{8} \text{Re Pr}}{1 + C \sqrt{\frac{\xi}{8}} (\text{Pr} - 1)}, \quad \text{Pr} \geq 0.5. \quad (7)$$

This equation was derived by Prandtl using a two-layer model of the boundary layer at the wall which consists of the laminar sublayer and the turbulent core. The constants C in Eq. (7) is equal to the dimensionless (friction) velocity at the hypothetical distance from the tube wall that is assumed to be the boundary separating laminar sublayer and turbulent core. The constant C depends on the thickness of the laminar sublayer assumed in the analysis and varies from $C = 5$ [1] to $C = 11.7$ [6]. Later Prandtl suggested that the constant C is equal to 8.7 [7].

The relation (7) was improved by Petukhov and Kirillov [6] using the Lyon integral [8,9] to obtain numerically the Nusselt number as a function of the Reynolds and Prandtl numbers. The eddy diffusivity of momentum and velocity profile in turbulent flow were calculated from experimental expressions given by Reichhardt [10]. The Lyon integral was evaluated numerically and the calculated Nusselt numbers were tabulated for various values of the Reynolds and Prandtl numbers. The obtained results can be approximated by different functions. Petukhov and Kirillov [9] suggested the following expression:

$$\text{Nu} = \frac{\frac{\xi}{8} \text{Re Pr}}{1.07 + 12.7 \sqrt{\frac{\xi}{8}} (\text{Pr}^{2/3} - 1)}, \quad 10^4 \leq \text{Re} \leq 5 \times 10^6, \quad 0.5 \leq \text{Pr} \leq 200, \quad (8)$$

where the friction factor for smooth tubes is given by

$$\xi = (1.82 \log \text{Re} - 1.64)^{-2}. \quad (9)$$

If the same data as for the Petukhov-Kirillov correlation (8) are used, then the following power-type correlation is obtained

$$\text{Nu} = 0.00685 \text{Re}^{0.904} \text{Pr}^{0.427}, \quad 10^4 \leq \text{Re} \leq 5 \times 10^6, \quad 0.5 \leq \text{Pr} \leq 200. \quad (10)$$

The Petukhov correlation (8) has been modified by Gnielinski [11,12] to the form

$$\text{Nu} = \frac{\frac{\xi}{8} (\text{Re} - 1000) \text{Pr}}{1.07 + 12.7 \sqrt{\frac{\xi}{8}} (\text{Pr}^{2/3} - 1)}, \quad 2.3 \times 10^3 \leq \text{Re} \leq 10^6, \quad 0.5 \leq \text{Pr} \leq 200. \quad (11)$$

to increase the accuracy of this equation in the transition area, i.e. in the range of Reynolds numbers: $2.3 \times 10^3 \leq \text{Re} \leq 10^4$. The relationships (5), (7), (8), (11), and (12) listed above were derived on the basis of heat transfer models for turbulent fluid flow in straight ducts and can be used for approximation of the experimental results in heat exchangers. However, the coefficients appearing in these correlations have to be adjusted using experimental data since the fluid flow path in heat exchangers is usually complex.

2 Experimental determination of heat transfer correlations

One of the most popular methods for determining the average heat transfer coefficients in heat exchangers is the Wilson plot method and its numerous modifications [3,13,14]. The Wilson method is based on the linear regression analysis of the experimental data. The disadvantage of the Wilson plot technique is the need to maintain constant thermal resistance of one of the fluids. Application of the method is limited to the power type correlations for Nusselt numbers. It is also difficult to apply Wilson's method for determining the average heat transfer coefficients in finned heat exchangers. In this paper, a general method for determining the average heat transfer coefficients in heat exchangers based on nonlinear least-squares method will be presented. A mathematical model of the heat exchanger is required that allows calculation of the heat exchanger outlet temperatures of both fluids assuming that mass flow rates and inlet temperatures of both fluids are known.

Unknown coefficients in heat transfer correlations will be determined based on measured mass flow rates and measured inlet and outlet temperatures of both fluids. These coefficients will be adjusted in such a way that the sum of squares of measured and calculated temperature at the outlet of the heat exchanger is minimum. The proposed method will be presented in detail on the example of determining the correlation for air and water

Nusselt numbers for a car radiator, which is a two-row tube and a plate fin heat exchanger with two passes.

2.1 Tested plate fin and tube heat exchanger

The tested automotive radiator is used for cooling the spark ignition engine of a cubic capacity of 1580 cm³. The cooling liquid, warmed up by the engine is subsequently cooled down by air in the radiator. The radiator consists of 38 tubes of an oval cross-section, with 20 of them located in the upper pass with 10 tubes per row (Fig. 1).

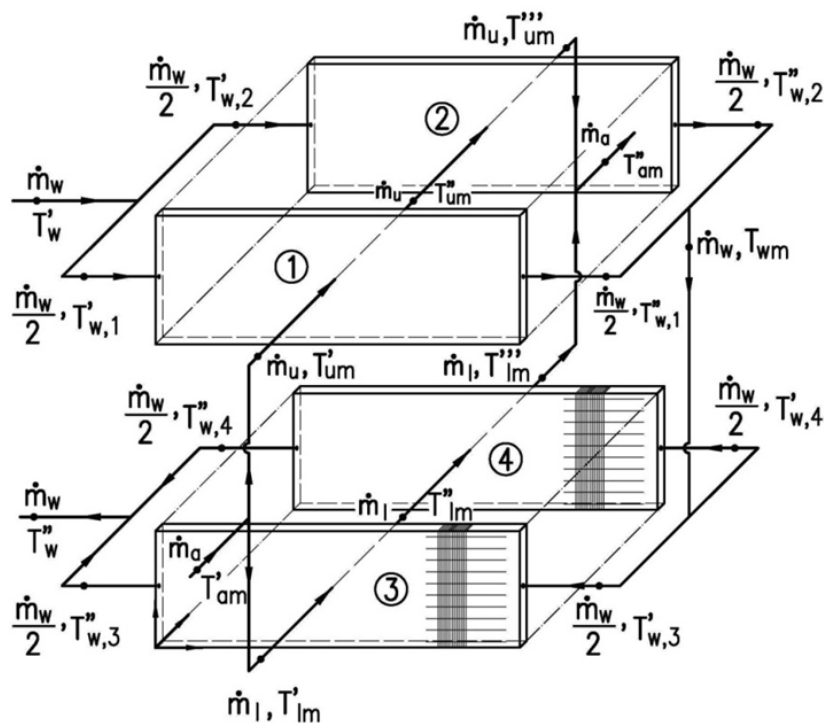


Figure 1. Flow diagram of two row cross-flow heat exchanger (automotive radiator) with two passes; 1 – first tube row in upper pass, 2 – second tube row in upper pass, 3 – first tube row in lower pass, 4 – second tube row in lower pass.

In the lower pass, there are 18 tubes with 9 tubes per row. The radiator is 520 mm wide, 359 mm high and 34 mm thick. The outer diameters of the oval tube are $d_{\min} = 6.35$ mm, $d_{\max} = 11.82$ mm. The tubes are

$L_{ch} = 0.52$ m long. The thickness of the tube wall is $\delta_t = 0.4$ mm. The number of plate fins equals to 520. The dimensions of the single tube plate are as follows: length – 359 mm, height – 34 mm and thickness – $\delta_f = 0.08$ mm. The plate fins and the tubes are made of aluminium. The path of the coolant flow is U -shaped. The two rows of tubes in the first pass are fed simultaneously from one header. The water streams from the first and second row are mixed in the intermediate header. Following that, the water is uniformly distributed between the tubes of the first and second row in the second pass. The inlet, intermediate and outlet headers are made of plastic. The pitches of the tube arrangement are as follows: perpendicular to the air flow direction $p_1 = 18.5$ mm and longitudinal $p_2 = 17$ mm. A smooth plate fin is divided into equivalent rectangular fins. Efficiency of the fin given by Eq. (7) was calculated by means of the finite element method. The hydraulic diameter of an oval tube is calculated using the formula $d_t = 4 A_{w,in}/P_{in}$. The Reynolds and Nusselt numbers were determined on the base of the hydraulic diameter, d_t . Equivalent hydraulic diameter, d_h , on the side of the air was calculated using the definition given by Kays and London [15]. Flow arrangement and construction of the radiator are discussed in detail in the monograph [16].

2.2 Experimental data

The heat transfer data were taken for cooling of hot water flowing through the car radiator. The experimental test facility and measurement procedure are presented in [16]. The following parameters are known from the measurements: water volumetric flow rate \dot{V}'_w , air velocity w_0 , water inlet and outlet temperature $(T'_w)^m$ and $(T''_w)^m$, air inlet and outlet temperature $(T'_{am})^m$ and $(T''_{am})^m$. Data were obtained for the series of four air velocities, spanning the range 1.0 to 2.2 m/s (Tab. 1).

The energy balance between the hot water and cold air sides was found to be within four percent for all runs (Tab. 2). The heat flow rates were calculated from the relations

$$\dot{Q}_{w,i} = \dot{V}'_{w,i} \cdot \rho_w [(T'_{w,i})^m] \cdot c_w \left| \frac{(T'_{w,i})^m}{(T''_{w,i})^m} \cdot [(T'_{w,i})^m - (T''_{w,i})^m] \right|, \quad (12)$$

$$\dot{Q}_{a,i} = \dot{V}'_{a,i} \cdot \rho_{a,i} [(T'_{am})^m] \cdot c_{pa} \left| \frac{(T''_{am})^m}{(T'_{am})^m} \cdot (T''_{am} - T'_{am}) \right|, \quad (13)$$

where

$$\dot{V}'_{a,i} = H_{ch} L_{ch} w_{0,i}. \quad (14)$$

Table 1. Measurement data.

i	$w_{0,i}$ [m/s]	$\dot{V}'_{w,i}$ [L/h]	$(T'_{w,i})^m$ [°C]	$(T''_{w,i})^m$ [°C]	$(T'_{am,i})^m$ [°C]	$(T''_{am,i})^m$ [°C]
1	1.00	872.40	71.08	61.83	15.23	54.98
2	1.00	949.20	70.76	62.07	14.89	55.31
3	1.00	1025.40	70.51	62.35	14.74	55.64
4	1.00	1103.40	70.30	62.65	14.59	56.03
5	1.00	1182.60	70.18	62.91	14.65	56.39
6	1.00	1258.80	69.99	63.18	14.87	56.75
7	1.00	1335.00	69.79	63.33	14.87	56.90
8	1.00	1408.80	69.68	63.51	14.71	57.15
9	1.00	1488.60	69.48	63.67	14.86	57.33
10	1.00	1564.80	69.25	63.73	14.81	57.45
11	1.00	1642.20	69.01	63.77	14.78	57.53
12	1.00	1714.80	68.82	63.83	14.77	57.53
13	1.00	1797.00	68.60	63.85	14.97	57.66
14	1.00	1892.40	68.35	63.83	14.98	57.65
15	1.00	1963.80	67.57	63.26	14.65	57.14
16	1.00	2041.20	66.96	62.80	14.24	56.72
17	1.00	2116.20	66.86	62.77	14.17	56.68
18	1.00	2190.60	66.73	62.83	14.27	56.75
19	1.27	865.80	66.33	56.74	14.11	49.56
20	1.27	942.60	66.16	56.96	13.91	49.69
21	1.27	1020.00	66.00	57.40	14.21	50.28
22	1.27	1099.20	65.82	57.66	13.91	50.60
23	1.27	1176.00	65.76	58.01	13.76	51.03
24	1.27	1252.20	65.68	58.27	13.63	51.42
25	1.27	1329.00	65.51	58.43	13.94	51.76
26	1.27	1404.00	65.46	58.71	13.83	52.02
27	1.27	1478.40	65.36	58.95	14.02	52.34
28	1.27	1557.60	65.25	59.12	13.88	52.52
29	1.27	1631.40	65.14	59.25	13.78	52.68
30	1.27	1708.80	65.05	59.35	13.58	52.83
31	1.27	1789.20	65.02	59.55	13.48	53.06
32	1.27	1882.20	65.02	59.80	13.49	53.23
33	1.27	2040.00	64.70	59.80	13.40	53.50
34	1.27	2118.00	64.70	59.80	13.40	53.41
35	1.27	2188.80	64.73	60.14	13.42	53.61
36	1.77	863.40	63.93	52.22	13.17	42.85
37	1.77	1015.80	63.65	53.18	13.21	44.23
38	1.77	1173.60	63.57	54.15	13.18	45.43
39	1.77	1249.20	63.53	54.60	13.09	45.92
40	1.77	1327.80	63.40	54.86	13.14	46.34
41	1.77	1476.60	63.36	55.44	13.00	47.11
42	1.77	1630.80	63.34	56.05	13.03	47.87
43	1.77	1789.80	63.25	56.52	13.14	48.37
44	1.77	1959.00	63.14	56.91	13.03	48.86
45	1.77	2112.60	62.91	57.10	13.00	49.12
46	1.77	2186.40	62.89	57.26	13.00	49.32
47	2.20	865.20	62.28	49.58	13.12	38.51
48	2.20	1017.00	62.24	50.64	12.91	39.83
49	2.20	1171.80	62.09	51.53	12.80	41.03

i	$w_{0,i}$ [m/s]	$\dot{V}'_{w,i}$ [L/h]	$(T'_{w,i})^m$ [°C]	$(T''_{w,i})^m$ [°C]	$(T'_{am,i})^m$ [°C]	$(T''_{am,i})^m$ [°C]
50	2.20	1251.00	61.96	51.93	12.73	41.62
51	2.20	1326.60	61.89	52.28	12.74	42.05
52	2.20	1476.60	61.65	52.85	12.73	42.82
53	2.20	1630.80	61.58	53.41	12.76	43.50
54	2.20	1788.00	61.39	53.82	12.73	44.06
55	2.20	1954.20	61.24	54.19	12.69	44.52
56	2.20	2109.60	61.18	54.56	12.69	44.94
57	2.20	2186.40	61.00	54.56	12.70	45.06

The relative difference between water side $\dot{Q}_{w,i}$ and average heat flow rate $\dot{Q}_{m,i}$ was evaluated as follows

$$\varepsilon_i = \frac{\dot{Q}_{w,i} - \dot{Q}_{m,i}}{\dot{Q}_{m,i}} \cdot 100, \quad (15)$$

where

$$\dot{Q}_{m,i} = \frac{\dot{Q}_{w,i} + \dot{Q}_{a,i}}{2}. \quad (16)$$

Using 57 experimental data sets listed in Tab. 2, the correlations for the air and tube side heat transfer coefficients were determined. Different correlations for air and water side were used and compared with each other. The construction of the heat exchanger and the materials of which it is made are also known.

3 Determining heat transfer correlations on the liquid and air sides

The estimation of the heat transfer coefficients of the air- and water-sides is the inverse heat transfer problem [17,18]. The following parameters are known from the measurements: water volumetric flow rate, \dot{V}'_w , at the inlet of the heat exchanger, air velocity w_0 before the heat exchanger, water inlet temperature $(T'_w)^m$, air inlet temperature, $(T'_{am})^m$, and water outlet temperature, $(T''_w)^m$. Next, specific forms of correlations were adopted for the Nusselt numbers on the air Nu_a and water Nu_w sides, containing $n \leq m$ unknown coefficients x_i $i = 1, \dots, n$. The coefficients x_1, x_2, \dots, x_n were

Table 2. Water $\dot{Q}_{w,i}$ and air $\dot{Q}_{a,i}$ side heat flow rates and relative difference ε_i between water side and average $\dot{Q}_{m,i}$ heat flow rates.

i	$\dot{Q}_{w,i}$ [W]	$\dot{Q}_{a,i}$ [W]	$\dot{Q}_{m,i} = (\dot{Q}_{w,i} + \dot{Q}_{a,i}) / 2$ [W]	$\varepsilon_i = \frac{\dot{Q}_{w,i} - \dot{Q}_{m,i}}{\dot{Q}_{m,i}} 100$ [%]
1	9186.2	9031.1	9108.7	0.9
2	9390.6	9194.0	9292.3	1.1
3	9526.4	9307.8	9417.1	1.2
4	9610.8	9436.8	9523.8	0.9
5	9789.2	9502.6	9645.9	1.5
6	9761.0	9526.6	9643.8	1.2
7	9820.4	9560.9	9690.6	1.3
8	9898.3	9660.4	9779.3	1.2
9	9849.3	9661.9	9755.6	1.0
10	9837.4	9702.8	9770.1	0.7
11	9801.1	9727.8	9764.4	0.4
12	9746.7	9730.4	9738.5	0.1
13	9723.4	9708.1	9715.8	0.1
14	9744.6	9703.4	9724.0	0.2
15	9645.5	9673.9	9659.7	-0.1
16	9679.1	9684.6	9681.9	0.0
17	9866.3	9694.3	9780.3	0.9
18	9739.1	9683.2	9711.2	0.3
19	9470.8	10266.2	9868.5	-4.0
20	9891.9	10369.5	10130.7	-2.4
21	10006.3	10443.4	10224.9	-2.1
22	10232.0	10634.0	10433.0	-1.9
23	10396.8	10808.5	10602.6	-1.9
24	10584.9	10963.0	10773.9	-1.8
25	10734.2	10959.5	10846.9	-1.0
26	10811.4	11071.9	10941.7	-1.2
27	10811.1	11102.3	10956.7	-1.3
28	10892.9	11200.1	11046.5	-1.4
29	10962.7	11279.3	11121.0	-1.4
30	11112.6	11388.9	11250.8	-1.2
31	11165.9	11490.1	11328.0	-1.4
32	11209.3	11536.0	11372.6	-1.4
33	11405.5	11645.0	11525.2	-1.0
34	11841.6	11617.7	11729.6	1.0
35	11462.9	11668.4	11565.6	-0.9
36	11545.4	12015.9	11780.6	-2.0
37	12145.1	12557.8	12351.5	-1.7
38	12624.0	13058.8	12841.4	-1.7
39	12738.0	13297.4	13017.7	-2.1
40	12948.5	13446.3	13197.4	-1.9
41	13353.8	13822.1	13588.0	-1.7
42	13574.7	14117.2	13846.0	-2.0
43	13753.7	14269.2	14011.5	-1.8
44	13935.7	14517.4	14226.5	-2.0
45	14016.1	14637.8	14326.9	-2.2
46	14056.2	14717.9	14387.1	-2.3
47	12556.6	12780.4	12668.5	-0.9
48	13480.4	13558.7	13519.6	-0.3

i	$\dot{Q}_{w,i}$ [W]	$\dot{Q}_{a,i}$ [W]	$\dot{Q}_{m,i} = (\dot{Q}_{w,i} + \dot{Q}_{a,i}) / 2$ [W]	$\varepsilon_i = \frac{Q_{w,i} - Q_{m,i}}{Q_{m,i}} 100$ [%]
49	14139.5	14226.0	14182.8	-0.3
50	14337.8	14563.4	14450.6	-0.8
51	14567.5	14771.2	14669.4	-0.7
52	14848.6	15165.5	15007.0	-1.1
53	15224.9	15494.8	15359.9	-0.9
54	15467.2	15791.3	15629.3	-1.0
55	15744.1	16046.0	15895.1	-0.9
56	15959.4	16259.4	16109.4	-0.9
57	16091.6	16315.5	16203.5	-0.7

estimated using the weighted least squares method

$$S = \sum_{i=1}^m \frac{[(T''_{w,i})^m - (T''_{w,i})^c]^2}{\sigma_{w,i}^2} + \sum_{i=1}^m \frac{[(T''_{am,i})^m - (T''_{am,i})^c]^2}{\sigma_{a,i}^2} = \min, \quad (17)$$

where the calculated water and air outlet temperatures are functions of measured values and unknown parameters, i.e.

$$(T''_{w,i})^c = (T''_{w,i})^c \left[(\dot{V}'_{w,i}, T'_{w,i}), (w_{0,i}, T'_{am,i}), x_1, x_2, \dots, x_n \right], \quad (18)$$

$$(T''_{am,i})^c = (T''_{am,i})^c \left[(\dot{V}'_{w,i}, T'_{w,i}), (w_{0,i}, T'_{am,i}), x_1, x_2, \dots, x_n \right]. \quad (19)$$

The sum of squared differences (18) between measured and calculated values of water and air at the outlet of the heat exchanger can be expressed in the compact form as

$$S(\mathbf{x}) = \{(\mathbf{T}'')^m - [\mathbf{T}''(\mathbf{x})]^c\}^T \mathbf{W} \{(\mathbf{T}'')^m - [\mathbf{T}''(\mathbf{x})]^c\}, \quad (20)$$

$$(\mathbf{T}'')^m = [(T''_{w,1})^m, (T''_{w,2})^m, \dots, (T''_{w,m})^m, (T''_{am,1})^m, (T''_{am,2})^m, \dots, (T''_{am,m})^m]^T, \quad (21)$$

$$(\mathbf{T}'')^c = [(T''_{w,1})^c, (T''_{w,2})^c, \dots, (T''_{w,m})^c, (T''_{am,1})^c, (T''_{am,2})^c, \dots, (T''_{am,m})^c]^T. \quad (22)$$

$$\mathbf{W} = \begin{bmatrix} w_{w,1} & \cdots & 0 & 0 & \cdots & 0 \\ 0 & \cdots & & & & \\ & & w_{w,m} & & & \vdots \\ \vdots & & & w_{a,1} & \cdots & 0 \\ 0 & \cdots & & 0 & w_{a,m} & \end{bmatrix}_{2m \times 2m}, \quad (23)$$

where the weighting factors $w_{w,i}$ and $w_{a,i}$ are equal to the inverses of the variances of the measured water and air values of temperature at the outlet of the heat exchanger, i.e. $w_{w,i} = 1/\sigma_{w,i}^2$, $w_{a,i} = 1/\sigma_{a,i}^2$, $i = 1, \dots, m$.

The parameters x_1, x_2, \dots, x_n for which the sum (21) is minimum are determined by the Levenberg-Marquardt method [19] using the following iteration

$$\mathbf{x}^{(k+1)} = \mathbf{x}^{(k)} + \delta^{(k)}, \quad k = 1, \dots \quad (24)$$

where

$$\delta^{(k)} = \left[\left(\mathbf{J}^{(k)} \right)^T \mathbf{W} \mathbf{J}^{(k)} + \mu^{(k)} \mathbf{I}_n \right]^{-1} \left(\mathbf{J}^{(k)} \right)^T \mathbf{W} \left\{ \left(\mathbf{T}'' \right)^m - \left[\mathbf{T}'' \left(\mathbf{x}^{(k)} \right) \right]^c \right\}. \quad (25)$$

The Jacobian matrix \mathbf{J} is given by

$$\mathbf{J} = \frac{\partial \mathbf{T}^c(\mathbf{x})}{\partial \mathbf{x}^T} = \left[\left(\frac{\partial T_i^c(\mathbf{x})}{\partial x_j} \right) \right]_{2m \times n}, \quad i = 1, \dots, 2m, \quad j = 1, \dots, n. \quad (26)$$

The partial derivatives in the Jacobian matrix

$$\mathbf{J} = \begin{bmatrix} \frac{\partial (T''_{w,1})^c}{\partial x_1} & \frac{\partial (T''_{w,1})^c}{\partial x_2} & \cdots & \frac{\partial (T''_{w,1})^c}{\partial x_n} \\ \vdots & \vdots & \vdots & \vdots \\ \frac{\partial (T''_{w,m})^c}{\partial x_1} & \frac{\partial (T''_{w,m})^c}{\partial x_2} & \cdots & \frac{\partial (T''_{w,m})^c}{\partial x_n} \\ \frac{\partial (T''_{am,1})^c}{\partial x_1} & \frac{\partial (T''_{am,1})^c}{\partial x_2} & \cdots & \frac{\partial (T''_{am,1})^c}{\partial x_n} \\ \vdots & \vdots & \vdots & \vdots \\ \frac{\partial (T''_{am,m})^c}{\partial x_1} & \frac{\partial (T''_{am,m})^c}{\partial x_2} & \cdots & \frac{\partial (T''_{am,m})^c}{\partial x_n} \end{bmatrix}_{2m \times n} \quad (27)$$

were calculated using the finite difference method.

The symbol \mathbf{I}_n designates the identity matrix of $n \times n$ dimension, and $\mu^{(k)}$ the weight coefficient, which changes in accordance with the algorithm suggested by Levenberg and Marquardt. The upper index T denotes the transposed matrix. After a few iteration we obtain a convergent solution.

4 Water and air temperature at heat exchanger outlet

The water temperature $(T''_{w,i})^c$ and air temperature $(T''_{am,i})^c$ at the outlet of the heat exchanger appearing in weighted sum of squares (18) can be calculated using the analytical or numerical models [16,20] of the heat exchanger or the number of transfer units (NTU) method [1,3]. In this paper, the outlet water temperature (Fig. 1) is calculated from the analytical expression [20]

$$(T''_w)^c = T''_w = \frac{T''_{w,3} + T''_{w,4}}{2}, \quad (28)$$

where the outlet water temperature $(T''_{w,3})^c$ from the first row in the lower pass, and the outlet water temperature $(T''_{w,4})^c$ from the second row in the lower pass are given by

$$T''_{w,3} = T'_{am} + (T_{wm} - T'_{am}) \exp \left\{ -\frac{N''_w}{N''_a} \left[(1 - \exp(-N''_a)) \right] \right\}, \quad (29)$$

$$T''_{w,4} = T'_{am} + [C_l + (T_{wm} - T'_{am})] \exp(-B_l). \quad (30)$$

The symbol T_{wm} denotes the mean water temperature between the first and second pass (Fig. 1). This temperature is equal to calculated as the arithmetic mean from the outlet water temperature $T''_{w,1}$ and $T''_{w,2}$ (Fig. 1)

$$T_{wm} = \frac{T''_{w,1} + T''_{w,2}}{2}, \quad (31)$$

where the water temperatures $T''_{w,1}$ and $T''_{w,2}$ are calculated from the following expressions:

$$T''_{w,1} = T'_{am} + (T'_w - T'_{am}) \exp \left\{ -\frac{N''_w}{N''_a} \left[(1 - \exp(-N''_a)) \right] \right\}, \quad (32)$$

$$T''_{w,2} = T'_{am} + [C_u + (T'_w - T'_{am})] \exp(-B_u). \quad (33)$$

The mean air temperature $(T''_{am})^c$ after the heat exchanger is given by

$$(T''_{am})^c = T''_{am} = \frac{n_u}{n_r} T'''_{um} + \frac{n_l}{n_r} T'''_{lm}. \quad (34)$$

The mean air temperature behind the first (upper) T'''_{um} and the second (lower) pass T'''_{lm} are

$$T'''_{um} = T'_{am} + (T'_w - T'_{am}) \left\{ \frac{1 - \exp(-2N_a^u)}{B_u} [1 - \exp(-B_u)] + [1 - \exp(-N_a^u)]^2 \left[\frac{1 - \exp(-B_u)}{B_u} - \exp(-B_u) \right] \right\}, \quad (35)$$

$$T'''_{lm} = T'_{am} + (T'_w - T'_{am}) \left\{ \frac{1 - \exp(-2N_a^l)}{B_l} [1 - \exp(-B_l)] + [1 - \exp(-N_a^l)]^2 \left[\frac{1 - \exp(-B_l)}{B_l} - \exp(-B_l) \right] \right\}, \quad (36)$$

where

$$B_u = \frac{N_w^u}{N_a^u} [1 - \exp(-N_a^u)], \quad B_l = \frac{N_w^l}{N_a^l} [1 - \exp(-N_a^l)], \quad (37)$$

$$C_u = B_u (T'_w - T'_{am}) [1 - \exp(-N_a^u)], \quad (38)$$

$$C_l = B_l (T'_w - T'_{am}) [1 - \exp(-N_a^l)],$$

$$N_w^u = \frac{U_u A_u^I}{\frac{\dot{m}_w}{2} \bar{c}_w} = \frac{2 U_u A_u^I}{\dot{m}_w \bar{c}_w}, \quad N_w^l = \frac{U_l A_l^I}{\frac{\dot{m}_w}{2} \bar{c}_w} = \frac{2 U_l A_l^I}{\dot{m}_w \bar{c}_w}, \quad (39)$$

$$N_a^u = \frac{U_u A_u^I}{\dot{m}_u \bar{c}_a} = \frac{U_u A_u^I}{\frac{n_u}{n_r} \dot{m}_a \bar{c}_a} = \frac{n_r U_u A_u^I}{n_u \dot{m}_a \bar{c}_a}, \quad (40)$$

$$N_a^l = \frac{U_l A_l^I}{\dot{m}_l \bar{c}_a} = \frac{U_l A_l^I}{\frac{n_l}{n_r} \dot{m}_a \bar{c}_a} = \frac{n_r U_l A_l^I}{n_l \dot{m}_a \bar{c}_a},$$

$$\bar{c}_w = c_w \left| \frac{T''_w}{T''_w} \right|, \quad \bar{c}_a = c_a \left| \frac{T''_{am}}{T''_{am}} \right|, \quad (41)$$

$$n_r = n_u + n_l, \quad A_u^I = A_u^{II} = n_u A_{to} = n_u P_o L_c, \quad A_l^I = A_l^{II} = n_l A_{to} = n_l P_o L_c. \quad (42)$$

The overall heat transfer coefficient U_o is related to the outer surface of the bare tube A_o

$$\frac{1}{U_o} = \frac{1}{h_o (h_a)} + \frac{A_o}{A_m} \frac{\delta_t}{k_t} + \frac{A_o}{A_{in}} \frac{1}{h_w}, \quad (43)$$

where the symbol h_o designates the weighted heat transfer coefficient defined as

$$h_o = h_a \left[\frac{A_{mf}}{A_o} + \frac{A_f}{A_o} \eta_f (h_a) \right]. \quad (44)$$

Since the conditions at the water and air side are identified simultaneously, the determined correlations account for the real flow arrangement and construction of the heat exchanger. As can be seen, expressions for the fluid outlet temperatures are of complicated form. For this reason, in the case of heat exchangers with complex structure and complex flow arrangements, it is better to calculate the outlet temperature of fluid by the effectiveness-number of transfer units (NTU) method or by the effectiveness-number of transfer units (P-NTU) method [3]. The ε -NTU or P-NTU formulas have been obtained in the recent past for many complicated flow arrangements [3]. In the case of new heat exchangers with complex structure is highly recommendable the use of numerical modeling to calculate the outlet temperature of the fluids [16,20,22].

5 Uncertainty analysis

The uncertainties for the estimated parameters were determined using the Gauss variance propagation rule [19,21]. Confidence intervals of the determined parameters in the correlations for the heat transfer coefficients at the sides of the air and water. The real values of the determined parameters $\tilde{x}_1, \dots, \tilde{x}_n$ are found with the probability of $P = (1 - \alpha) 100\%$ in the following intervals:

$$x_i - t_{2m-n}^{\alpha/2} s_t \sqrt{c_{ii}} \leq \tilde{x}_i \leq x_i + t_{2m-n}^{\alpha/2} s_t \sqrt{c_{ii}}, \quad (45)$$

where

- x_i – parameter determined using the least squares method,
- $t_{2m-n}^{\alpha/2}$ – quantile of the t -Student distribution for the confidence level $100(1 - \alpha)\%$ and $2m - n$ degrees of freedom.

The least squares sum is characterized by the variance of the fit s_t^2 , which is an estimate of the variance of the data σ^2 and is calculated according to

$$s_t^2 = \frac{1}{2m-n-1} \left\{ \sum_{i=1}^m \frac{[(T''_{w,i})^m - (T''_{w,i})^c]^2}{\sigma_{w,i}^2} + \sum_{i=1}^m \frac{[(T''_{am,i})^m - (T''_{am,i})^c]^2}{\sigma_{a,i}^2} \right\} \min, \quad (46)$$

$$\frac{1}{2m} \sum_{i=1}^m \left(\frac{1}{\sigma_{w,i}^2} + \frac{1}{\sigma_{a,i}^2} \right)$$

where $2m -$ denotes the number of measurement points, and $n -$ stands for the number of searched parameters.

The weighting factors $w_{w,i} = 1/\sigma_{w,i}^2$ or $w_{a,i} = 1/\sigma_{a,i}^2$ are the inverses of the variances $\sigma_{w,i}^2$ and $\sigma_{a,i}^2$ which describe the uncertainties of the data

points for water or air and are normalized to the average of all the weighting factors. If the Levenberg-Marquardt iterative method is used to solve the nonlinear least-squares problem, then the estimated variance-covariance matrix from the final iteration is

$$\mathbf{D}_x^{(s)} = s_t \mathbf{C}_x^{(s)} = s_t \left[\left(\mathbf{J}^{(s)} \right)^T \mathbf{W} \mathbf{J}^{(s)} \right]^{-1}, \quad (47)$$

where the matrix $\mathbf{C}_x^{(s)}$ is

$$\mathbf{C}_x^{(s)} = \left[\left(\mathbf{J}^{(s)} \right)^T \mathbf{W} \mathbf{J}^{(s)} \right]^{-1}. \quad (48)$$

The superscript (s) denotes the number of the last iteration while \mathbf{J} is the Jacobian matrix.

The symbol c_{ii} in Eq. (45) denotes the diagonal element c_{ii} of the matrix $\mathbf{C}_x^{(s)}$.

In this paper, the following values are under consideration: $m = 57$ (Tab. 1), and $n = 4$. Quantiles $t_{m-n}^{\alpha/2}$ and $t_{2m-n}^{\alpha/2}$ for 95% confidence level ($\alpha = 0.05$) are: $t_{53}^{0.025} = 2$ and $t_{110}^{0.025} = 2$. Having solved the nonlinear least squares problem, the temperature differences of the calculated and measured outlet temperatures are known. Next, the minimum of the sum S_{min} of the squared temperature differences given by Eq. (18) and the 95% confidence intervals can be calculated from Eq. (45).

6 Results and discussion

Initially, a specific form of correlation equations is assumed for nondimensional heat transfer coefficients at the side of the air

$$\text{Nu}_a = h_a d_h / k_a = \text{Nu}_a (\text{Re}_a, \text{Pr}_a, x_1, \dots, x_{n_a}) \quad (49)$$

and at the side of the water

$$\text{Nu}_w = h_w d_t / k_w = \text{Nu}_w (\text{Re}_w, \text{Pr}_w, x_{n_a+1}, \dots, x_n), \quad (50)$$

where the symbol n_a is the number of unknown parameters in the air side correlation and $(n - n_a)$ is the number of unknown parameters in the water side correlation. The Reynolds and Nusselt numbers were determined based

on the hydraulic diameters. Equivalent hydraulic diameters on the side of the air, d_h , and the fluid, d_t , are defined as follows:

$$d_h = \frac{4 A_{\min} L}{A'_f + A'_{mf}}, \quad (51)$$

$$d_t = \frac{4 A_{w, in}}{P_{in}}, \quad (52)$$

where the fin surface of a single passage, A'_f , and the tube outside surface between two fins, A'_{mf} , are given by (Fig. 2)

$$A'_f = 2 \cdot 2 (p_1 p_2 - A_{oval}) = 4 (p_1 p_2 - A_{oval}), \quad A'_{mf} = 2 A_{mf} = 2 P_o (s - \delta_f). \quad (53)$$

The minimum cross-section area for transversal air flow through the tube array, related to one tube pitch, p_1 , is (Fig. 2)

$$A_{\min} = (s - \delta_f) (p_1 - d_{\min}). \quad (54)$$

The air-side Reynolds number $Re_a = w_{\max} d_h / \nu_a$ in the correlation (49) is based on the maximum fluid velocity, w_{\max} , occurring within the tube row, and is defined by (Fig. 2)

$$w_{\max} = \frac{s p_1}{(s - \delta_f) (p_1 - d_{\min})} \frac{\bar{T}_{am} + 273}{T'_{am} + 273} w_0, \quad (55)$$

where w_0 is the air velocity before the radiator. The temperatures \bar{T}_{am} and T'_{am} are in °C.

As the tubes in the radiator are set in line, w_{\max} is the air velocity in the passage between two tubes. The thermophysical properties of the hot water were determined at the mean temperature $\bar{T}_w = (T'_w + T''_w) / 2$, where T'_w and T''_w denote the inlet and outlet temperatures. All properties appearing in the Eq. (55) for the air are also evaluated at the mean air temperature $\bar{T}_{am} = (T'_{am} + T''_{am}) / 2$ (Fig. 1).

Based on the analysis conducted in the first section the air correlation (49) was assumed in the form of the Colburn equation and four different forms of Eq. (50) are selected (Tab. 3). The correlations are valid for

$$150 \leq Re_a \leq 350, \quad 4000 \leq Re_w \leq 12000.$$

The correlations (56)–(59) in Tab. 3 are based only on the measured water temperatures ($m = 57$) at the outlet of the heat exchanger while correlations

Table 3. Correlations for air and water side Nusselt numbers for the automotive radiator.

Correlation	Weights	Estimated parameters
$\text{Nu}_a = x_1 \text{Re}_a^{x_2} \text{Pr}_a^{1/3}$ $\text{Nu}_w = x_3 \text{Re}_w^{0.8} \text{Pr}_w^{1/3} \left[1 + \left(\frac{d_t}{L_{ch}} \right)^{2/3} \right]$ (56)	$w_{ww,i=1}$ $w_{a,i=0}$ $i=1, \dots, m$	$s_t = 0.1022 \text{ K}$ $x_1 = 0.0640 \pm 0.0114$ $x_2 = 0.7876 \pm 0.0335$ $x_3 = 0.0161 \pm 0.0207$
$\text{Nu}_a = x_1 \text{Re}_a^{x_2} \text{Pr}_a^{1/3}$ $\text{Nu}_w = x_3 \text{Re}_w^{0.9} \text{Pr}_w^{0.43} \left[1 + \left(\frac{d_t}{L_{ch}} \right)^{2/3} \right]$ (57)	$w_{w,i} = 1$ $w_{a,i} = 0$ $i = 1, \dots, m$	$s_t = 0.0993 \text{ K}$ $x_1 = 0.0814 \pm 0.0010$ $x_2 = 0.7307 \pm 0.0137$ $x_3 = 0.0066 \pm 0.0448$
$\text{Nu}_a = x_1 \text{Re}_a^{x_2} \text{Pr}_a^{1/3}$ $\text{Nu}_w = \frac{\frac{24}{\sigma_w} (Re_w - x_3) \text{Pr}_w}{1 + x_4 \sqrt{\frac{\sigma_w}{\sigma_a}} (\text{Pr}_w - 1)} \left[1 + \left(\frac{d_t}{L_{ch}} \right)^{2/3} \right]$ (58)	$w_{w,i} = 1$ $w_{a,i} = 0$ $i = 1, \dots, m$	$s_t = 0.0981 \text{ K}$ $x_1 = 0.0988 \pm 0.0081$ $x_2 = 0.6741 \pm 0.0152$ $x_3 = 1422 \pm 0.1949$ $x_4 = 6.22 \pm 0.1990$
$\text{Nu}_a = x_1 \text{Re}_a^{x_2} \text{Pr}_a^{1/3}$ $\text{Nu}_w = \frac{\frac{24}{\sigma_w} (Re_w - x_3) \text{Pr}_w}{1 + x_4 \sqrt{\frac{\sigma_w}{\sigma_a}} (\text{Pr}_w^{2/3} - 1)} \left[1 + \left(\frac{d_t}{L_{ch}} \right)^{2/3} \right]$ (59)	$w_{w,i} = 1$ $w_{a,i} = 0$ $i = 1, \dots, m$	$s_t = 0.0980 \text{ K}$ $x_1 = 0.0899 \pm 0.0028$ $x_2 = 0.6990 \pm 0.0060$ $x_3 = 1079 \pm 0.1974$ $x_4 = 16.38 \pm 0.1998$
$\text{Nu}_a = x_1 \text{Re}_a^{x_2} \text{Pr}_a^{1/3}$ $\text{Nu}_w = \frac{\frac{\sigma_w}{\sigma_a} (Re_w - x_3) \text{Pr}_w}{1 + x_4 \sqrt{\frac{\sigma_w}{\sigma_a}} (\text{Pr}_w^{2/3} - 1)} \left[1 + \left(\frac{d_t}{L_{ch}} \right)^{2/3} \right]$ (60)	$w_{w,i} = 100$ $(\sigma_{w,i} = 0.1)$ $w_{a,i} = 1$ $(\sigma_{a,i} = 1)$ $i = 1, \dots, m$	$s_t = 0.1207 \text{ K}$ $x_1 = 0.0852 \pm 0.0014$ $x_2 = 0.7116 \pm 0.0032$ $x_3 = 1145 \pm 0.2327$ $x_4 = 16.17 \pm 0.2428$
$\text{Nu}_a = x_1 \text{Re}_a^{x_2} \text{Pr}_a^{1/3}$ $\text{Nu}_w = \frac{\frac{\sigma_w}{\sigma_a} (Re_w - x_3) \text{Pr}_w}{1 + x_4 \sqrt{\frac{\sigma_w}{\sigma_a}} (\text{Pr}_w^{2/3} - 1)} \left[1 + \left(\frac{d_t}{L_{ch}} \right)^{2/3} \right]$ (61)	$w_{w,i} = 1$ $(\sigma_{w,i} = 1)$ $w_{a,i} = 0.01$ $(\sigma_{a,i} = 10)$ $i = 1, \dots, m$	$s_t = 0.1207 \text{ K}$ $x_1 = 0.0850 \pm 0.0046$ $x_2 = 0.7121 \pm 0.0102$ $x_3 = 1144 \pm 0.2439$ $x_4 = 16.22 \pm 0.2446$

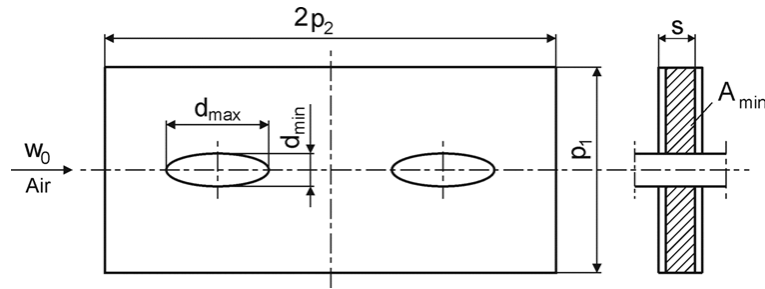


Figure 2. Cross section of two parallel tubes in the heat exchanger illustrating determination of the equivalent hydraulic diameter on the air side.

(60) and (61) are based on measured water and air temperatures. The confidence intervals of the coefficients x_1, \dots, x_4 are small, which results from a good accuracy of the developed mathematical model of the radiator and small measurement errors.

Figures 3 and 4 compare the correlations listed in Tab. 3.

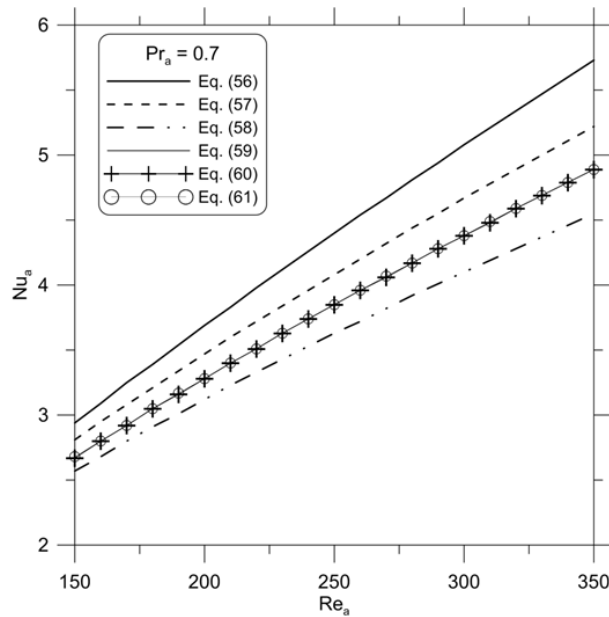


Figure 3. Comparison of correlations from Table 3 for air side Nusselt number.

Figures 3 and 4 show that when power type correlations (56) and (57) are used for water then the power type correlations for air overpredict the air

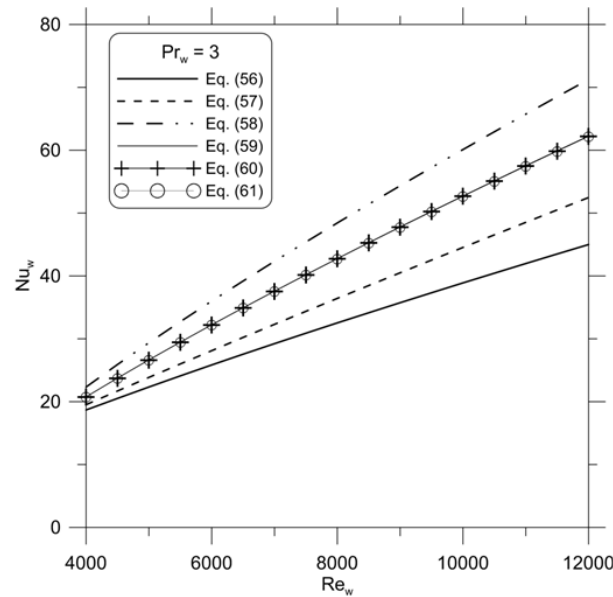


Figure 4. Comparison of correlations from Tab. 3 for water side Nusselt number.

side Nusselt numbers which were obtained when the Nusselt type correlation (58) or Petukhov-Gnielinski type correlations (59)–(61) were used as the correlations for water. However, if the exponent to the water side Reynolds number Re_w in the relation (57) is equal to 0.9 as in the correlation (11), then the agreement of the correlation (57) with other correlations from Tab. 3 is better. It can be seen from Figs 3 and 4 that if the air side heat transfer coefficient is too large, then the water side heat transfer is too low and vice versa when the heat transfer coefficient on the water side is too large a heat transfer coefficient on the air side is too small. It should be emphasized that regardless of heat transfer coefficients on the water and air side, the overall heat transfer coefficient, U_o , is always the same. Comparison of correlations (60) and (61) shows that the determined coefficients are almost identical. This is due to the same ratio of the weighting factors on the water and air side, which is equal to $w_{w,i}/w_{a,i} = \sigma_{a,i}^2/\sigma_{w,i}^2 = 100$, $i = 1, \dots, m$.

For the correct determination of the correlations for Nusselt numbers on the air and water side it is sufficient to take into account only outlet water temperatures in the sum of the squares. This is due to greater accuracy in measuring the water side heat flow rate because the mass flow rate and inlet

and outlet temperatures can be measured with high accuracy. The measurement of the heat flow rate on the air side is less accurate due to the difficulty of accurate measuring of the air mass flow rate and mass average air temperature (bulk mean temperature) behind the heat exchanger. The mass average temperature is a temperature that is averaged over cross section of the flow duct weighted by the local flow velocity. Thus, the measurement of the mass average velocity requires the simultaneous measurement of the velocity and temperature over the passage cross section. The air outlet temperatures can be included in the sum of the squares provided the relative differences ε_i , between the experimentally determined water and mean flow rates are very small, for example, for $\varepsilon_i \leq 2\%$, $i = m + 1, \dots, 2m$.

7 Conclusions

In the paper, a new method for the simultaneous determination of the heat transfer correlations for both fluids has been presented. The method is based on the weighted least squares method. In the sum of squared differences between measured and computed outlet fluid temperatures, both water and air temperatures are taken into account. Because of the lower accuracy of measurement of the air volumetric flow rate and mass average air temperature after the heat exchanger, is recommended to use in the sum of the squares higher weighting factors for the temperature differences on the water side. The proposed method allows estimation of the 95% confidence intervals of determined parameters. The method can be used to determine the unknown coefficients in the Nusselt number correlations of any form. The paper presents an example application of the method for determining the heat transfer correlations on the air and water side in a plate fin-and-tube heat exchanger.

The developed method can be applied to various types of heat exchangers. To determine the outlet temperatures of both fluids analytical and numerical methods can be used. Fluid outlet temperatures can also be relatively quickly and easily determined by the ε -NTU or P-NTU method.

Received 1 August 2012

References

- [1] WELTY J.R., WICKS CH.E., WILSON R.E., RORRER G.L.: *Fundamentals of Momentum, Heat, and Mass Transfer*, 5th edn. John Wiley & Sons, New York 2007.

- [2] MCADAMS W.H.: *Heat Transmissions*, 3rd edn. McGraw-Hill, New York 1954.
- [3] SHAH R. K., SEKULIĆ D.P.: *Fundamentals of Heat Exchanger Design*. Wiley, Hoboken 2003.
- [4] DITTUS F.W., BOELTER L.M.K.: *Heat transfer in automobile radiators of the tubular type*. University of California Publ. on Eng. **2**(1930), 443–461, reprinted in: Int. Commun. Heat Mass Transfer **12**(1985), 3–22.
- [5] PRANDTL L.: *Eine Beziehung zwischen Wärmeaustausch und Strömungswiderstand der Flüssigkeit*. Z. Physik, **11**(1910), 1072–1078.
- [6] PETUKHOV B.S., GENIN A.G., KOVALEV S.A.: *Heat Transfer in Nuclear Power Plants*. Atomizdat, Moscow 1974 (in Russian).
- [7] PRANDTL L.: *Führer durch die Strömungslehre*. Vieweg und Sohn, Braunschweig 1944.
- [8] LYON R.N.: *Liquid metal heat transfer coefficients*. Chem. Engr. Progr. **47**(1951), 2, 75–79.
- [9] KUTATELADZE S.S.: *Fundamentals of Heat Transfer*. Edward Arnold, London 1963.
- [10] REICHHARDT H.: *Vollständige Darstellung der turbulenten Geschwindigkeitsverteilung in glatten Leitungen*. Angew. Math. Mech. **30**(1951), 7, 208–219.
- [11] GNIELINSKI V.: *Neue Gleichungen für den Wärme- und den Stoffübergang in turbulent durchströmten Rohren und Kanälen*. Forschung im Ingenieurwesen **41**(1975), 1, 8–16.
- [12] GNIELINSKI V.: *New equations for heat and mass transfer in turbulent pipe and channel flow*. Int. Chem. Engng. **16**(1976), 359–368.
- [13] WILSON E.E.: *A basis for rational design of heat transfer apparatus*. Trans. ASME **37**(1915), 47–70.
- [14] WEBB R.L., NARAYANAMURTHY R., THORS P.: *Heat transfer and friction characteristics of internal helical-rib roughness*. Trans. ASME, J. Heat Transfer **122**(2000), 134–142.
- [15] KAYS W.M., LONDON A.L.: *Compact Heat Exchangers*. McGraw-Hill, 3rd edn. New York 1984.
- [16] TALER D.: *Dynamics of Tube Heat Exchangers*. AGH University of Science and Technology Press, Cracow 2009 (in Polish).
- [17] TALER D.: *Methods for obtaining heat transfer correlations for plate finned heat exchangers using experimental and CFD simulated data*. Arch. Thermodynamics **25**(2004), 4, 31–54.
- [18] TALER D.: *Experimental and numerical predictions of the heat transfer correlations in the cross-flow plate fin and tube heat exchangers*. Arch. Thermodynamics **28**(2007), 2, 3–18.
- [19] SEBER G.A.F., WILD C.J.: *Nonlinear Regression*. Wiley, New York 1989.
- [20] TALER D.: *Theoretical and experimental analysis of heat exchangers with extended surfaces*. Cracow Branch of Polish Academy of Sciences, Automotive Committee, Cracow, Poland 2002, Vol. 25, Monograph 3.

-
- [21] BEVINGTON P.R.: *Data Reduction and Error Analysis for the Physical Sciences*. McGraw-Hill, New York 1969.
- [22] TALER D., TROJAN M., TALER J.: *Numerical modeling of cross-flow tube heat exchangers with complex flow arrangements*. In: *Evaporation, Condensation and Heat Transfer*, Amimul Ahsan Ed., Chap. 13, 261–278. InTech, Rijeka-Shanghai 2011.